

# Classical Dynamics Simulation of Projectile–Surface Interactions

M. A. Karolewski\*

Division of Information Technology and Strategy, Nanyang Technological University, Nanyang Avenue, Singapore 639798

A public-domain package of programs for the personal computer, the *Simulation Kit* (SK), has been developed for the simulation and visualization of collisions of low-energy (<10 keV) atomic projectiles with solid target lattices. Possible applications of the SK include the simulation of ion scattering spectra, sputtering coefficients, reflection coefficients and projectile ranges. The simulation model used by the SK is based on classical dynamics, and uses a composite screened-Coulomb/Morse pair potential to model interactions between particles in the target. The simulation model also incorporates inelastic scattering effects based on the Lindhard–Schjøtt–Scharff, Oen–Robinson and Shapiro–Tombrello models, respectively. The physical basis of the simulation model is described, and examples are provided of applications in ion beam analysis (ion scattering spectrometry, sputter yields). Copyright © 1998 John Wiley & Sons, Ltd.

KEYWORDS: computer simulation; ion scattering; sputtering; atomic collisions

## INTRODUCTION

The interaction of energetic projectiles with solids forms the basis of several surface analysis techniques, such as ion scattering spectroscopy (ISS),<sup>1</sup> secondary ion mass spectrometry (SIMS)<sup>2</sup> and ion-induced Auger electron emission.<sup>3</sup> Atomic bombardment phenomena also play significant roles in many modern industries, including microelectronics, nuclear energy and the space industry.

The microscopic interpretation of atomic scattering experiments on solids is increasingly based on computer simulations that have been carried out in many laboratories during the past three decades. Comprehensive reviews of the techniques used for computer simulation of atomic collisions in solids (including state-of-art methods) can be found in the books by Eckstein and by Smith *et al.*<sup>4,5</sup> Historically, simulation efforts have led to the emergence of two distinct computational approaches: the binary collision approximation (BCA) model<sup>6</sup> and the classical dynamics (CD) model.<sup>7</sup> The BCA model treats a collision sequence as a series of classical binary collisions, and normally only follows scattering events in which one of the collision partners is initially at rest (neglecting any overlap of recoil trajectories). In contrast, the CD model treats the collision system as a classical many-particle ensemble, and takes into account multiple interactions involving both projectile and target atoms. The strength of the BCA model lies in its speed, while that of the CD model is its greater accuracy, particularly in modelling many-particle interactions at low energies.

Numerous BCA and CD programs for simulation of scattering processes in solid lattices or amorphous matter have been developed, and several of these have

been released by their authors into the public domain.<sup>4,5,8,9</sup> The most established BCA programs, such as MARLOWE and TRIM, can be executed on many platforms, including personal computers.<sup>10</sup> Typically, the public domain CD programs are intended for use with minicomputers or mainframe computers, and require some programming knowledge to build and use;<sup>11</sup> a recent exception is KSCAN, which runs on Macintosh personal computers.<sup>10</sup>

This paper introduces a personal computer software package designed for CD simulations of atomic collisions in solid lattices. The suite of programs is collectively known as the *Simulation Kit* (SK). The intended audience is the experimental ion beam analysis community. The SK comprises an integrated group of software tools for the design, execution and analysis of *ad hoc* CD simulation projects on a production basis. The SK's graphical user interfaces also incorporate facilities for real-time or post-simulation visualization of atomic collision simulation results, either as snapshots or as cinematic sequences. The investment of time required to master the use of some existing CD or BCA programs presents a significant barrier to experimental groups who may wish to use them for interpretation and modelling of their own ion beam analysis data. Accordingly, the need for user acceptance of the SK programs has been an important consideration during their development, and a number of modifications have been made as a result of feedback from users of preliminary versions of the package. The SK package is freely distributable, and may be obtained by anonymous file transfer through the Internet.<sup>12</sup>

The SK is based on a multiple-interaction dynamical model, in which interactions between particles in a crystalline lattice are represented by composite pair potentials.<sup>13</sup> One advantage of CD models based on pair potentials is the ability to parameterize both the repulsive and attractive regions of interatomic potentials in universal forms. Typical applications of the SK are in: sputtering (angular and energy dependences, statistics)

\* Correspondence to: M. A. Karolewski, Block 8, Hillview Avenue 08-1210, Singapore 661008.

E-mail: akarol@ntu.edu.sg

and projectile scattering (cross-sections, backscattering coefficients, ranges). The SK can also be used for modelling discrete and continuous electronic stopping processes. Although pair potential models can provide quantitative descriptions of a wide range of energetic atomic scattering phenomena, they do not provide accurate descriptions of very low-energy interactions (e.g. those determining state functions) in transition metals and semiconductors, for which the local bonding environment must be incorporated into the interaction model.<sup>14–16</sup> This limitation disqualifies the SK for studies of the equilibrium energetics of structural phases, particularly those that involve large changes in atomic coordination or density relative to the undisturbed lattice. Although many-body potentials presumably allow more accurate trajectory calculations than pair potentials, the influence of many-body effects on measurable dynamic processes such as sputtering may not be significant in practice.<sup>17</sup>

The purpose of this report is to outline the functions and capabilities of the SK, to benchmark the package and provide illustrative examples of applications in ion beam analysis and, lastly, to indicate some future directions for development.

---

## COMPUTER IMPLEMENTATION

---

The physical model, and the assumptions underlying the CD simulations performed by the SK and similar codes, are described in detail in the literature,<sup>4,5,13</sup> and in the SK package documentation, and will only be presented in outline here. The physical parameters used for each SK simulation are specified in a series of six input files (designated respectively as the *target*, *projectile*, *model*, *run*, *impact* and *inelastic* input files) that are generated by an interactive utility program (SPIDER) according to the requirements of the user. The input data are distributed among several files in order to facilitate the reuse of input files when a single aspect of the simulation is changed during batch runs (e.g. the projectile energy or its angle of incidence). The setting up of a typical simulation problem requires the specification of about 50 numeric input parameters.

The *target* and *projectile* input files, respectively, specify the target and projectile characteristics. The target would normally consist of a cluster or a lattice of atomic particles, numbering in the region of 1000–2000 particles for sputtering or trajectory studies, or 10–40 particles for angle-resolved projectile backscattering studies (the maximum permitted number is 30 000).

The *run* input file specifies the kind of output that is to be generated by the simulation, and miscellaneous details about the way in which the simulation is to be executed and terminated. The output data generated by a simulation consist of a listing of the dynamical variables (position, momentum and other information) of selected particles at a given stage (elapsed time) of the simulation and, optionally, a catalogue of inelastic energy-loss events. No processing of this information is carried out until the simulation is finished.

Projectile–target and target–target interaction potential parameters are specified in the *model* input file, as are the parameters needed for (optional) inclusion of

thermal vibration effects. The projectile–target interaction is described by means of a Molière or Ziegler–Biersack–Littmark (ZBL) screened-Coulomb potential.<sup>4,18</sup> The interaction between atoms in the target is modelled using a screened-Coulomb potential at short internuclear separations ( $r$ ) and a Morse potential at large separations. Tabulations of Morse potential parameters from the literature are provided,<sup>19,20</sup> but users may deviate from these if they choose. A cubic polynomial spline function joins the two potentials in an intermediate region. The interaction potentials are cut off at a finite distance specified by the user (normally beyond the first or second lattice neighbour distance). A planar surface potential optionally may be included at the target lattice boundaries. The SK also provides an option for ignoring target–target interactions. This ‘partial’ CD simulation option is useful for modelling energetic projectile backscattering processes that occur on a short timescale, because it speeds up calculations with virtually no effect on accuracy.<sup>21</sup>

The *impact* input file defines the grid of projectile incident trajectories. This grid, which is generally rectangular or triangular in shape, maps to a symmetry-reduced zone of the target surface that is normally smaller in extent than the surface unit cell.<sup>7,22</sup>

Lastly, the *inelastic* input file specifies how inelastic (electronic loss) effects are to be incorporated into the simulation. The following inelastic-loss models are supported: Lindhard–Schjøtt–Scharff (LSS),<sup>23,24</sup> Oen–Robinson<sup>25</sup> and Shapiro–Tombrello.<sup>26</sup> These inelastic-loss models may be used singly, in arbitrary combination or not at all.

The SK’s simulation module (named SNOOK) is implemented in a manner that closely follows the methodology described by Smith and Harrison,<sup>13</sup> with the following differences: the SK does not employ the moving-atom approximation;<sup>27</sup> look-up tables are only used to calculate the Morse (not the screened-Coulomb) forces; inelastic energy-loss effects (see above) may optionally be incorporated into the dynamical model used by the SK.

The user of the SK may select any of several integration algorithms,<sup>13</sup> of which the Verlet algorithm is the normal choice. After the establishment of initial conditions, the equations of motion of the dynamical system are integrated repeatedly over many time-steps until one of the user-defined termination conditions (based on elapsed time and maximum particle kinetic energy) is met. The accuracy of the integration method, which depends primarily on the selected time-step, is monitored by the accuracy of energy conservation: the latter is typically arranged to be ~0.5% or less on average. Neighbour lists and a variable time-step are used to improve the speed of the simulation, in the manner described by Smith and Harrison.<sup>13</sup>

At the conclusion of the simulation, the stored trajectory information can be examined and manipulated using a dedicated utility program (WINNOW), or it can be converted to ascii text format for loading into a spreadsheet or other data-processing application. Typically, the first operation on the output data is that of transferring a selected portion of the output to a second file (e.g. data referring to a specific particle in the system, or for a selected range of particle energies or emission angles). The WINNOW program permits the

**Table 1.** *Simulation Kit* calculation of the average elastic energy losses ( $\Delta E$ ) and root-mean-square angular deflections ( $\Delta\theta$ ) suffered by projectiles passing through thin crystalline targets (nine monolayers of Si(100) and five monolayers of Cu(100), respectively), compared with the results of a round-robin study (RR) that examined the performance of six established CD codes<sup>29</sup>

System	$\Delta E$ (eV), this work	$\Delta E$ (eV), RR	$\Delta\theta$ (°), this work	$\Delta\theta$ (°), RR
0.2 keV B–Si(100)	66.1	63.1–68.4	35.2	32.6–34.5
0.5 keV B–Si(100)	64.6	55.9–65.1	25.7	22.1–25.1
1.0 keV Ar–Cu(100)	424.9	412.1–428.4	19.6	19.1–19.8

use of custom filter expressions, comparable to those used by relational database applications, which facilitate operations of this kind. The WINNOWER program is able to generate binned distributions of *ad hoc* functions of dynamical variables (typically energy spectra or angular/spatial distributions) from simulation output files. The program also offers a number of statistical averaging and data formatting options, which are likewise constructed from user-defined expressions.

The pair potential formalism used by the SK is most apt for the description of scattering processes in elemental targets. However, scattering processes that are dominated by the repulsive core potentials, such as ion scattering spectrometry, can be modelled by the SK for targets of arbitrary composition. The SK can also be applied for other purposes (with varying degrees of realism) to compound target systems that satisfy certain subsidiary conditions. For example, scattering processes in binary compounds composed of atoms with similar electronic shells (e.g. CuNi or GaAs) can be modelled on the assumption that the same long-range (attractive) interaction holds for all atoms. Compound systems with arbitrary constituents are more difficult to treat consistently within the SK methodology in the attractive potential region. One possible strategy is to neglect the attractive portion of the adsorbate–substrate and adsorbate–adsorbate pair interactions entirely, but to include a planar surface potential that is applied only to adsorbate particles. A system of logical control flags is provided in the SK for this and other specialized applications, but the usefulness of such compromises needs to be evaluated on a case-by-case basis because there may be no advantage compared to a BCA calculation. Limitations such as these are inherent in any pair potential model, and can only be overcome by using a new interaction formalism such as that provided by the embedded-atom method.<sup>28</sup>

## BENCHMARKS

As with most complex software, it is difficult in general to formally prove or estimate the correctness of a CD simulation code under all circumstances. The dynamical system should accurately conserve momentum, angular momentum and energy, respectively, in elastic scattering processes. Other tests of correctness that can be used during program development include the comparison of scattering angles, apsidal distances and energy losses calculated for two- and three-body systems with the corresponding values calculated by hand. The conservation of energy is perhaps the best indication at run-time

that the equations of motion have been integrated correctly for individual trajectories by the CD program, but this benchmark cannot detect systematic errors such as the failure to choose an appropriate sample of projectile impact parameters.<sup>7</sup>

There are relatively few benchmarks available in the atomistic simulation literature that serve to compare program performance and accuracy under controlled, realistic running conditions. Gärtner *et al.* recently reported the results of a round-robin comparison of six CD simulation programs and six BCA simulation programs.<sup>29</sup> The various programs were used to calculate the mean elastic energy losses and root-mean-square angular deflections suffered by a projectile passing through thin crystalline targets of Cu and Si, respectively. (The reader is referred to the original reference for specific details of the simulation problems.) The CD results from the round robin are compared with the corresponding results calculated using the SK (with the Verlet integration algorithm) in Table 1. The level of agreement between the SK results and the round-robin CD results is generally good, although two of the angular deflections computed by the SK fall just outside the range reported by the contributors to the round-robin study. The SK yielded similar results when the HGE-B integration algorithm was used instead of the Verlet algorithm;<sup>13</sup> this result supports the suggestion made in Ref. 29 that the small discrepancies that exist between the various CD codes examined are due to systematic differences in the methods used for impact parameter sampling or trajectory termination, rather than to integration errors.

Table 2 presents the results of a simple simulation exercise that the author has used to benchmark the SK against the well-known BCA code MARLOWE.<sup>6</sup> The simulations involved the estimation of elastic scattering

**Table 2.** Reflection coefficients ( $R$ ) calculated by the *Simulation Kit* (SK) and by the BCA program MARLOWE,<sup>30</sup> respectively, for 1 keV Ar projectiles incident on Cu(100) at various altitudinal angles ( $\phi$ ) in the  $\langle 011 \rangle$  plane

$\phi$ (°)	$R$ , SK	$R$ , MARLOWE
90	0.078	0.06
50	0.184	0.16
30	0.580	0.62

reflection coefficients for 1 keV Ar projectiles incident on an ideal Cu(100) surface at various altitudinal angles (30°, 50° and 90°, respectively) along a [011] azimuth. The SK simulation at each incident angle consisted of 1250 trajectories. Reflection coefficients were estimated by counting the number of projectiles found to be located  $>1$  Å above the surface with positive velocities after 80 fs had elapsed in the simulation. Table 2 shows that the reflection coefficients computed in this way by the SK are in agreement to within 0.02–0.04 with those computed by MARLOWE.<sup>30</sup>

## APPLICATIONS

### Impact collision ion scattering spectrometry

The first application of the SK to be discussed involves the simulation of an impact collision ion scattering spectrometry (ICISS) measurement. Impact collision ion scattering spectrometry is an important technique for surface structure determination.<sup>31</sup> In ICISS, the yield of projectiles backscattered (at, or near, 180°) from a target lattice is profiled as a function of the projectile altitudinal angle of incidence ( $\phi$ ). The experimental parameters of interest are the critical angles for backscattering, which are measured on the low-angle edges of the peaks in the ICISS angular profile.

The ICISS simulation discussed here examines the altitudinal anisotropy of the yield of He projectiles backscattered at 180° from the Cu(110) surface, for a primary energy of 1.5 keV and a  $\langle 112 \rangle$  azimuthal direction of incidence. Experimental ICISS measurements for this system have been reported by Spitzl *et al.*<sup>32</sup> Note that the simulations treat the backscattering of neutral projectiles, in contrast to the experimental measurements which detect backscattered ions. It should also be emphasized that CD simulations are not the normal choice for fitting initial trial structures to ICISS data, because of their high computational cost compared with BCA or other types of model calculations.<sup>33,34</sup>

The clean Cu(110) surface exhibits a slight surface reconstruction, which takes the form of a small inward relaxation of the surface layer with respect to the second layer ( $-\Delta d_{12} = 5\text{--}10\%$  or  $\sim 0.1$  Å).<sup>35–38</sup> There is also a smaller outward relaxation of the second layer with respect to the third layer, which will be ignored for the present purposes ( $\Delta d_{23} = 2\text{--}3\%$  or  $\sim 0.03$  Å). The simulations presented here will compare the scattering behaviour of the ideal unreconstructed surface with that of two hypothetical relaxed surfaces characterized by substantial inward and outward displacements ( $\Delta d_{12} = -0.3$  and  $+0.3$  Å, respectively) of the outermost Cu surface layer. The purpose of the discussion is not to examine the experimental system *per se*, but rather, to draw attention to the capabilities and limitations of the simulation model for interpretation of ICISS data. It should also be mentioned that the methodology outlined here would be equally applicable to ISS measurements involving arbitrary scattering angles.

The scattering geometry used for the CD simulation is shown in Fig. 1. A number of possible backscattering mechanisms are indicated symbolically by lines connecting the edges of shadowing atoms with the back-

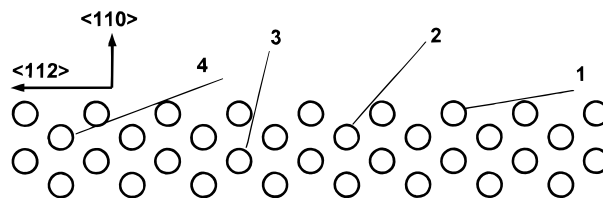


**Figure 1.** Symbolic representation of the major impact collision backscattering mechanisms for the  $\langle 112 \rangle$  scattering geometry for a (110) face-centred cubic lattice target. The figure depicts the structure in the plane of scattering, which is normal to the surface plane. Atomic positions are represented by circles. Straight lines connect the edges of shadowing atoms with the centres of back-scattering atoms.

scattering atom centres. The two-dimensional target consisted of 34 Cu atoms arranged into four rows in the plane of scattering. This planar simulation geometry is necessary to reduce computation time, because the probability of projectile backscattering after multiple collisions with non-coplanar atoms is negligible.<sup>31</sup>

Two kinds of simulations were carried out: full CD simulations (taking into account all interactions); and 'partial' CD simulations (ignoring all target–target interactions). The latter computations gave results that (to statistical accuracy) were indistinguishable from the former, yet were executed at more than twice their speed. For both sets of simulations, inelastic energy-loss effects were disregarded. For simulations of this nature, it is important that the repulsive part of the projectile–target interaction be realistic. The ZBL potential is based on fits to experimental measurements of nuclear stopping powers, and it appears on average to describe ISS shadowing data adequately without modification.<sup>39</sup> The close agreement between the Ar–Cu ZBL potential and the *ab initio* configuration interaction potential calculated by Broomfield *et al.*<sup>40</sup> has been noted elsewhere.<sup>41</sup> Nordlund *et al.* compared the ZBL potential for collision pairs involving light elements (H, C, N, Si) with potentials calculated using Hartree–Fock and density functional methods, and found agreement on average to within  $\sim 3\%$  for energies below 5 keV (and  $\sim 5\%$  for energies up to 10 keV).<sup>42</sup> Nevertheless, for this simulation a screening length correction of 0.9 was employed for the He–Cu ZBL interaction, because this appeared to produce a better description of the experimental data than the uncorrected potential. The Cu–Cu interactions in the full CD simulations were described by a composite Molière–Morse potential, joined by a cubic polynomial spline in the region  $r = 1.5\text{--}2.1$  Å. Both He–Cu and Cu–Cu potentials were cut off for  $r > 3.7$  Å. The Molière potential ( $r \leq 1.5$  Å) and Morse potential ( $2.1 \text{ Å} \leq r \leq 3.7 \text{ Å}$ ) parameters for the Cu–Cu interaction were taken from Table 4.6 of Eckstein's book.<sup>4</sup> The Cu–Cu spline potential function used in the intermediate region ( $1.5 \text{ Å} < r < 2.1 \text{ Å}$ ) was:  $V(r) = 584.5 - 741.7r + 310.3r^2 - 42.67r^3$ , where  $r$  is expressed in Å and  $V(r)$  in eV. Debeye–Waller vibrational displacements were randomly added to the lattice position of each target atom (in the plane of scattering only). If thermal vibration effects are not included in CD simulations of ICISS profiles, the scattering thresholds then appear as intense spikes rather than as broadened peaks. This approach is an acceptable simulation strategy if the purpose of the simulation is simply

to locate the critical angles.

For each incident altitudinal angle, 25 000 projectile trajectories were simulated. The projectile backscattering yield was estimated by counting the number of projectiles that were scattered through an angle of  $180 \pm 0.5^\circ$ , measured with respect to the incident projectile trajectory.

Simulations were performed at angular intervals of  $1^\circ$  in the vicinity of backscattering features, and  $3^\circ$  otherwise. Figure 2 compares the experimental ICISS angular profiles for this system<sup>32</sup> with simulated profiles for the ideal Cu(110) surface and for Cu(110) surfaces with outer layers contracted by 0.3 Å, or expanded by 0.3 Å, respectively. The numeric labels shown in Figs 1 and 2 indicate the correspondence between the scattering features in Fig. 2 and the backscattering mechanisms represented in Fig. 1.

It is apparent from visual inspection of Fig. 2 that the simulated data for the contracted Cu(110) surface give the best reproduction of the relative heights of the experimental scattering peaks, while the data for the expanded Cu(110) surface give the worst reproduction. Moreover, the calculations for the expanded surface show a peak or shoulder near  $\varphi = 21^\circ$ , although the experimental data show no feature of comparable intensity in this region. This peak was observed in both the

**Table 3.** Comparison of observed critical angles (in degrees) for ICISS peaks shown in Fig. 3 with the corresponding values calculated using the *Simulation Kit* (SK) under a variety of assumptions: (a) observed values from Ref. 32; (b) 0.3 Å contraction of Cu surface layer; (c) ideal Cu lattice; (d) 0.3 Å expansion of Cu surface layer

Peak	(a) Observed	(b) Contracted	(c) Ideal	(d) Expanded	(e) SCM
1	12.5	13.5	12.5	12.0	12.4
2	47.2	49.5	48.2	46.0	48.2
3	70.4	71.0	70.7	69.8	71.8

Data in columns (b)–(d) are calculated by CD simulation. Column (e) presents the corresponding values for the ideal Cu lattice, calculated with a single collision shadow-cone model (SCM). Estimated uncertainties in critical angle locations are  $\pm 0.5^\circ$  in columns (a)–(d) and  $\pm 0.1^\circ$  in column (e)

full and 'partial' CD simulations, and can be attributed to the increasing feasibility of the shadowing mechanism labelled as '4' in Fig. 1.

Table 3 compares the experimental and simulated critical backscattering angles derived from Fig. 2. Table 3 follows the convention of reading the critical angle positions at 85% of the respective peak intensities

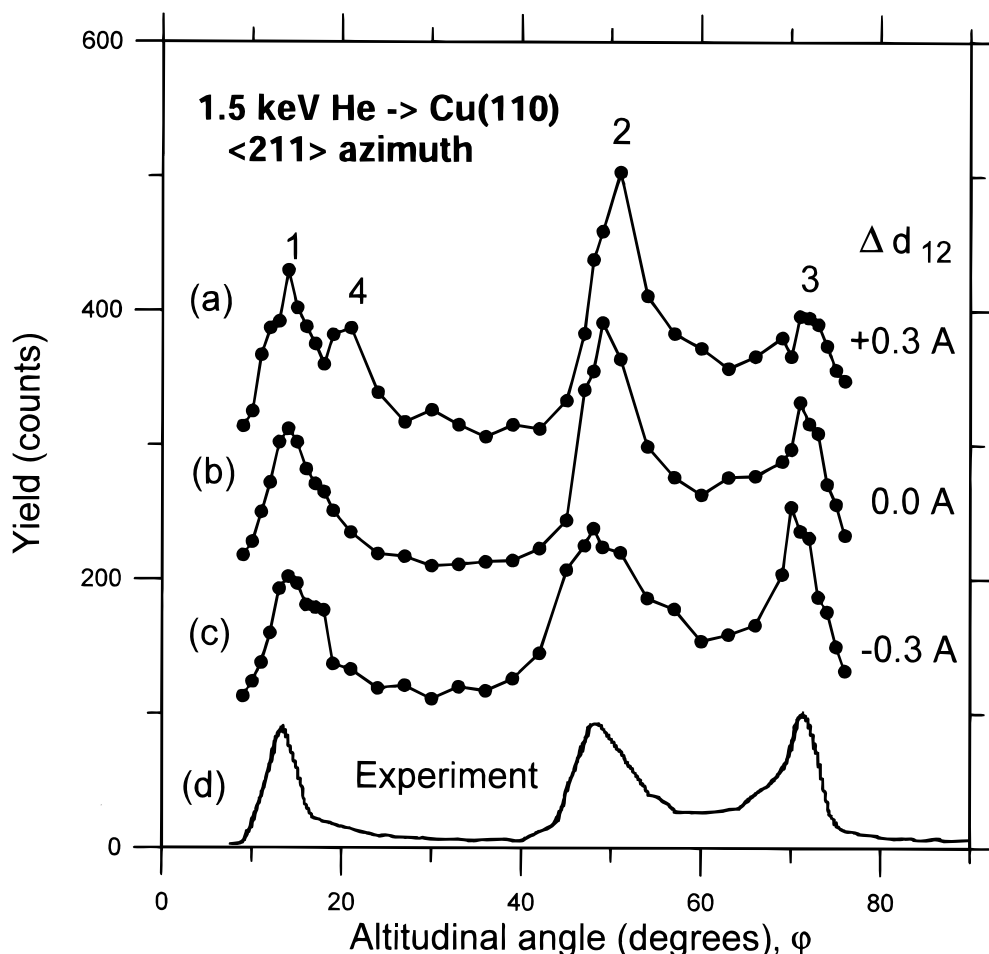


**Figure 2.** Comparison of simulated (a–c) and experimental (d) ICISS angular profiles for He projectiles backscattered from a Cu(110) target in the  $\langle 112 \rangle$  scattering geometry. The experimental data are taken from Ref. 32. The Cu target lattices used for the simulated data incorporate relaxation effects as follows: (a) 0.3 Å expansion of surface layer; (b) no relaxation (ideal lattice); (c) 0.3 Å contraction of surface layer. The backscattering yields for curves (a)–(c) are shifted upwards by multiples of 100 counts. The experimental peak intensity data, curve (d), have been arbitrarily rescaled.

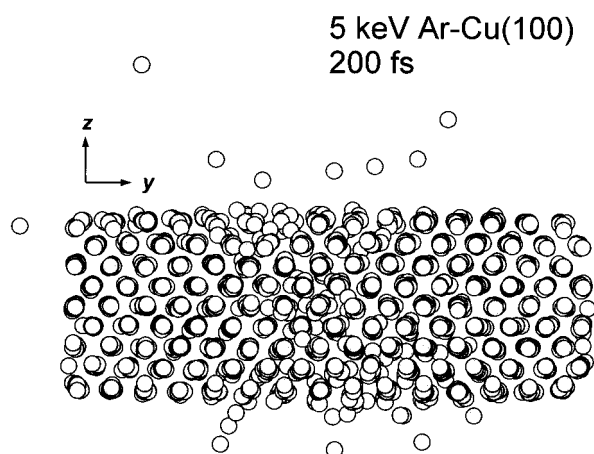


**Figure 3.** Lattice configuration resulting from a simulated impact of a 5 keV Ar projectile on a 2025 atom Cu(100) target after 200 fs have elapsed. The figure shows a projection of the positions of Cu atoms (represented by circles) onto the  $yz$  plane. The target surface lies in the  $xy$  plane. The projectile (which has left the depicted region) was incident in the  $-z$  direction, at an impact parameter of  $\sim 0.7$  Å with respect to the nearest surface Cu atom.

(measured relative to the background just below the peak).<sup>31</sup> The last column in Table 3 presents the corresponding critical angle estimates calculated using a single-collision shadow-cone model described previously.<sup>41</sup> The uncertainty in reading off the critical angles is reflected in the simulated results for peak 1 of Table 3. The critical angle for this in-surface scattering feature would not be expected to shift as a result of surface layer relaxation, yet the simulated results show a spread of  $1.5^\circ$ . This spread ( $\pm 0.75^\circ$ ) is comparable to the estimated uncertainties ( $\pm 0.5^\circ$ ), which arise both because of statistical effects and because there is a  $1^\circ$  interval between the projectile incident angles sampled by the simulation. This uncertainty can be reduced, in principle, with further computational effort.

The best agreement between the experimental and simulated critical angle data in Table 3 is found for the unreconstructed Cu lattice. However, the critical angle data listed in Table 3 are not in themselves sufficiently free of uncertainty as to warrant rejection of any of the three surface relaxation models considered here. Nevertheless, the substantial discrepancy in relative peak intensities between curves (a) and (d) of Fig. 2 and the absence of any significant experimental feature at  $\phi = 21^\circ$  can be used as a basis for rejecting the expanded-layer structure. In conclusion, the experimental ICISS data appear to be consistent with the results of the two remaining simulation models, implying a small (0.0–0.3 Å) or zero contraction of the outermost Cu(110) surface layer. In a real structural study of this surface, this result would need to be refined by carrying out further ICISS measurements and analyses along different azimuthal directions, according to the triangulation method used in Ref. 32.

Full or 'partial' CD simulations can be used in situations where a simple shadow-cone model fails to give satisfactory agreement with experimental ICISS measurements, but it would be impractical to use CD simulations in all circumstances. BCA calculations (if available) are considerably faster than CD calculations, yet have comparable accuracy for most ISS simulations, except in special cases where the projectile scattering

dynamics are influenced by multiple interactions, e.g. heavy or slow projectiles, or grazing angles of incidence. Classical dynamics simulations are computationally expensive and so are most useful for the final refinement of a structural model that has been established through other, faster methods.<sup>43,44</sup> For example, the shadow-cone model (Table 3) gives good estimates for the critical angles for the scattering systems considered here, with a systematic error (rather than uncertainty) of  $\sim 1^\circ$  or less. The shadow-cone model requires a negligible computational effort, but is limited in its ability to predict the critical angles for scattering events involving sub-surface atoms, e.g. mechanism 4 in Fig. 1.

### Sputtering

An important application of CD simulations has been the elucidation of sputtering mechanisms.<sup>7</sup> In principle, CD simulations give access to all aspects of the sputtering event, including the origins of sputtered atoms, the statistics of the sputtering process, the energy and angular distributions of sputtered atoms and the total sputter yield. Impact collision secondary ion mass spectrometry represents a practical surface analytical application of simulations of this type.<sup>45,46</sup> In the following example, the SK has been used to determine the variation of the sputtering coefficient (number of sputtered atoms per incident projectile) of a Cu(100) surface as a function of the projectile altitudinal angle. The projectile species in this simulation was 5 keV Ar. Experimental data<sup>47</sup> and calculated BCA results<sup>48</sup> have been presented for this problem. Sputtering of Cu(100) at normal projectile incidence has been investigated using a number of different CD simulation routines: a review of early work can be found in Ref. 7; more recent simulation approaches are described in Refs 26 and 49. Sputtering in the 5 keV Ar/Cu(111) system has been examined in detail using an embedded atom potential.<sup>50</sup> Once again, the purpose of the simulation presented here was to illustrate the capability of the SK programs, rather than to examine the physical system itself in detail.

The Cu target consisted of nine planes of Cu atoms, each plane consisting of 225 atoms (2025 atoms in total). This target configuration follows a prescription suggested by Harrison for absolute containment of collision cascades in the 5 keV Ar/Cu system.<sup>7</sup> Debeye-Waller vibrational displacements were randomly added to the lattice position of each target atom.<sup>51</sup> The 5 keV Ar projectile was incident on the surface in a direction parallel to the  $\langle 110 \rangle$  surface rows, at altitudinal angles ranging from  $20^\circ$  to  $90^\circ$ . The Ar-Cu interaction was represented by an uncorrected ZBL potential, while the Cu-Cu potential was based on the composite Molière-Morse potential described in the preceding section. Electronic energy-loss effects were taken into account by using an equipartition between the Lindhard-Schiøtt-Scharff and Oen-Robinson models, respectively. For each projectile angular configuration, 450 incident trajectories (directed into a rectangular symmetry zone based on the ideal lattice) were examined. The simulations were terminated after 200 fs had elapsed, by which time the majority of sputtered atoms had been ejected.<sup>13</sup> Atoms were considered to be sput-

tered if they had moved out of the surface interaction range and had a positive  $z$ -velocity at termination. The surface interaction range in this respect was specified as 4.0 Å (referenced to the ideal surface plane) by taking the sum of potential cut-off (3.7 Å) and twice the root-mean-square vibrational amplitude in the perpendicular direction (in total 0.27 Å).

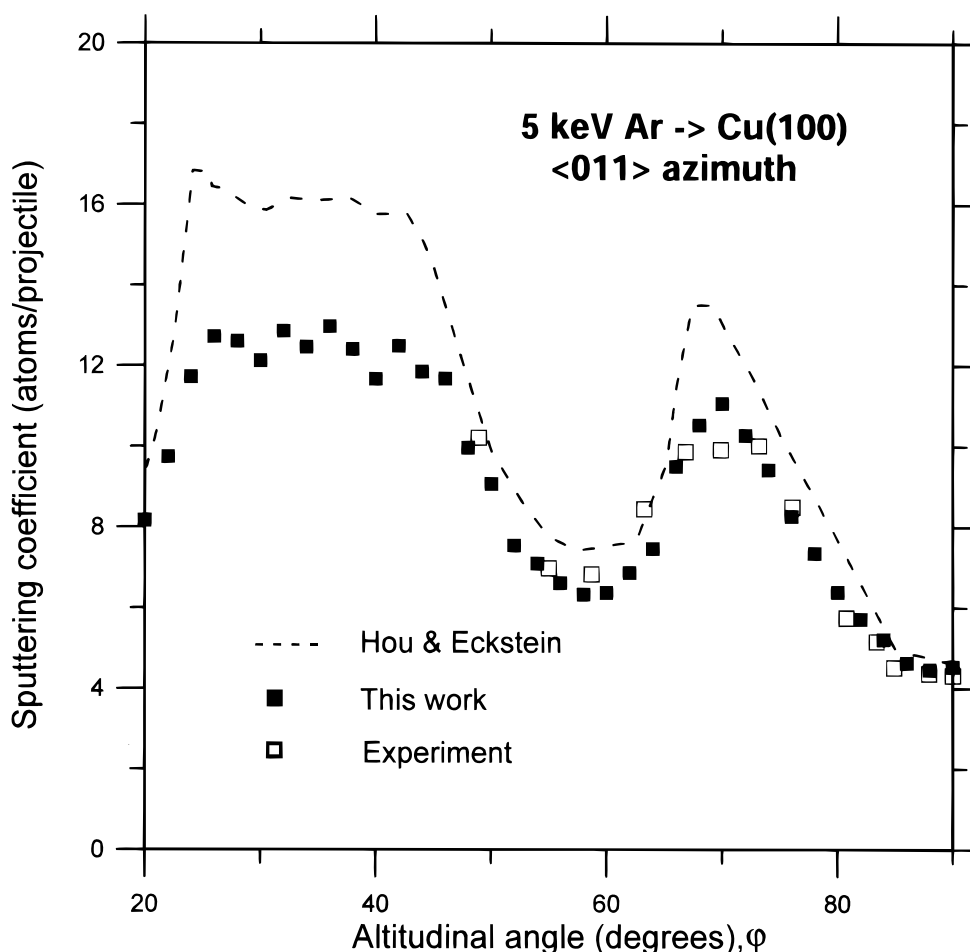
Figure 3 depicts a typical lattice configuration at termination. In this instance, lateral containment of the collision cascade at the surface is satisfactory (with the exception of one atom), but the depth of the lattice is apparently insufficient (at the bottom of Fig. 3) to contain the cascade vertically. For many projectile trajectories in this simulation, containment of the ensuing collision cascade in the bulk layers did not occur. However, these bulk containment effects do not propagate back to the surface, and therefore do not have a significant impact on the calculated sputter yields.<sup>7</sup>

Figure 4 presents the variation of the sputtering coefficient with projectile altitudinal angle of incidence. The plotted data compare the results of the SK computations with available experimental measurements of the sputtering coefficients,<sup>47</sup> and with BCA calculations of the sputtering coefficients performed by Hou and Eckstein.<sup>48</sup> The characteristic feature of the data shown in Fig. 4 is the presence of deep minima in the sputtering

coefficient, at incident angles that correspond to directions of high lattice transparency (i.e. the directions of major crystallographic axes). Projectiles incident in such directions tend to be steered gently into the target along the channels of the crystal lattice, depositing less of their energy in the surface region through hard collisions than randomly incident projectiles.<sup>48</sup> Channelling directions are therefore associated with an attenuated yield of sputtered atoms.<sup>6</sup> Both the SK and BCA calculations coincide with the experimental measurements near normal incidence. The SK gives good agreement with the measured sputtering coefficients across the angular range where experimental data are available. However, the BCA calculations appear to overestimate the sputter yield increase associated with the non-channelling direction near  $\phi = 70^\circ$ . Both computational approaches locate the sputter yield minima with satisfactory accuracy.

## CONCLUSIONS

The rapid development of microprocessors makes intensive scientific calculations on desktop computers increasingly feasible. A package of programs for the



**Figure 4.** The sputtering coefficient, shown as a function of the altitudinal angle of incidence, for bombardment of a Cu(100) surface by 5 keV Ar projectiles. The projectiles are incident in the  $\langle 011 \rangle$  plane. Black squares: sputtering coefficients calculated in this work. White squares: experimental sputtering coefficients from Ref. 47. The dashed line shows the sputtering coefficients calculated by Hou and Eckstein using the MARLOWE BCA program.<sup>48</sup>

design, execution and visualization of atomistic simulations on personal computers has been introduced in this paper. The purpose of the package is to facilitate production classical dynamics (CD) simulations of projectile-surface interactions. Users of the package need not necessarily be familiar with computer programming. The *Simulation Kit* (SK) should not only aid in the interpretation of data from established experiments, but may also prove useful in the development of new data collection methodologies. A number of potentially useful experimental measurements (e.g. angle-variation secondary ion mass spectrometry) are difficult to interpret without many-particle simulations. Indeed, the well-known ICISS experiment was devised initially as a response to the complexity of the interpretation of ion scattering patterns at arbitrary scattering angles.<sup>5,2</sup> Conversely, CD simulations can also be used to design scattering experiments (e.g. to estimate or optimize sensitivity). The SK may also serve as an introduction to the methodology of simulation for researchers who eventually intend to carry out their simulations in main-frame computing environments.

The pair-potential formalism used by the SK is not adequate to describe all atomistic phenomena relevant to surface characterization. Many-body potentials are demonstrably superior for studying low-energy solid-state properties such as point defects, surface reconstructions or state functions.<sup>16</sup> A natural development of the SK package would be to incorporate the capability of using many-body potentials, although this would likely be achieved at the cost of increased complexity for the user and reduced computation speed. Work towards this objective is currently in progress (based on the embedded-atom formalism)<sup>28</sup> and will be reported in due course.

### Acknowledgements

The author wishes to thank the numerous individuals who kindly commented on the preliminary releases of the *Simulation Kit*. The material support provided, respectively, by Professor R. G. Cavell (University of Alberta) and Dr D. Chadwick (Imperial College) in the early stages of this project is gratefully acknowledged.

### REFERENCES

1. J. W. Rabalais (ed.), *Low Energy Ion-Surface Interactions*. Wiley, Chichester (1994).
2. A. Benninghoven, F. G. Rudenauer and H. W. Werner, *Secondary Ion Mass Spectrometry*. Wiley, Chichester (1987).
3. S. Valeri, *Surf. Sci. Rep.* **17**, 85 (1993).
4. W. Eckstein, *Computer Simulation of Ion-Solid Interactions*. Springer-Verlag, Berlin (1991).
5. R. Smith, M. Jakas, D. Ashworth, B. Oven, M. Bowyer, I. Chakarov and R. Webb, in *Atomic and Ion Collisions in Solids and at Surfaces: Theory, Simulation and Applications*, edited by R. Smith. Cambridge University Press, Cambridge (1997).
6. M. T. Robinson, in *Sputtering by Particle Bombardment I: Physical Sputtering of Single Element Solids*, edited by R. Behrisch, p. 73. Springer-Verlag, Berlin (1981).
7. D. E. Harrison, *Radiat. Eff.* **70**, 1 (1983).
8. R. Smith and R. P. Webb, *Nucl. Instrum. Methods B* **67**, 373 (1992).
9. P. Sigmund *et al.*, *Nucl. Instrum. Methods B* **36**, 110 (1989).
10. Public domain atomic collision simulation programs can be obtained through the following Internet sites: MARLOWE: <http://www.ssd.ornl.gov/marlowe/marlowe.html>; SRIM (includes TRIM): <http://www.research.ibm.com/ionbeams/CRYSTAL-TRIM>; <http://www.fz-rossendorf.de/FWI/FWIT/ctrim.e.html>; MDRANGE: <http://beam.helsinki.fi/~knordlun/mdh/mdh-program.html>; KSCAN: <http://ksan.ms.nwu.edu/ksan.html>; TRIDYN: <http://www.cpc.cs.qub.ac.uk/cpc/>.
11. D. C. Rapaport, *Comput. Phys.* **4**, 337 (1997).
12. The *Simulation Kit* package, version 2.3, can be downloaded as the file 'simkit23.zip' from any of the following URLs: <ftp://ftp.simtel.net/pub/simtelnet/win95/science>; <ftp://src.doc.ic.ac.uk/packages/simtelnet/win95/science>; <http://oak.oakland.edu/pub/simtelnet/win95/science>.
13. R. Smith and D. E. Harrison, *Comput. Phys.* **3**, 68 (1988).
14. G. J. Ackland, G. Tichy, V. Vitek and M. W. Finnis, *Philos. Mag. A* **56**, 735 (1987).
15. G. J. Ackland and R. Thetford, *Philos. Mag. A* **56**, 15 (1987).
16. J. R. Smith and D. J. Srolovitz, *Modelling Simul. Mat. Sci. Eng.* **1**, 101 (1992).
17. M. H. Shapiro and T. A. Tombrello, *Nucl. Instrum. Methods B* **84**, 453 (1994).
18. I. M. Torrens, *Interatomic Potentials*. Academic Press, New York (1972).
19. L. A. Girifalco and V. G. Weizer, *Phys. Rev.* **114**, 687 (1959).
20. D. E. Harrison, *CRC Crit. Rev. Solid State Sci.* **14** (suppl. 1), 1 (1988).
21. M. Posselt and K.-H. Heinig, *Nucl. Instrum. Methods B* **102**, 236 (1995).
22. D. E. Harrison, C. E. Carlston and G. D. Magnuson, *Phys. Rev.* **139A**, 737 (1965).
23. J. Lindhard, M. Scharff and H. E. Schiøtt, *K. Dan. Vidensk. Selsk. Mat. Fys. Medd.* **33**, 14 (1966).
24. J. Lindhard and M. Scharff, *Phys. Rev.* **124**, 128 (1961).
25. O. S. Oen and M. T. Robinson, *Nucl. Instrum. Methods* **132**, 647 (1976).
26. M. H. Shapiro and T. A. Tombrello, *Nucl. Instrum. Methods B* **94**, 186 (1994).
27. R. Smith, D. E. Harrison and B. J. Garrison, *Phys. Rev. B* **40**, 93 (1989).
28. S. M. Foiles, M. Baskes and M. S. Daw, *Phys. Rev. B* **33**, 7983 (1986).
29. K. Gärtner *et al.*, *Nucl. Instrum. Methods B* **102**, 183 (1995).
30. M. Hou and M. T. Robinson, *Nucl. Instrum. Methods* **132**, 641 (1976).
31. H. Niehus, W. Heiland and E. Taglauer, *Surf. Sci. Rep.* **17**, 213 (1993).
32. R. Spitzl, H. Niehus and G. Comsa, *Surf. Sci. Lett.* **250**, L355 (1991).
33. R. S. Williams, Quantitative Intensity Analysis of Low-Energy Scattering and Recoiling from Crystal Surfaces, in *Low Energy Ion-Surface Interactions*, pp. 1-54, and references therein. Wiley, Chichester (1994).
34. M. H. Langelaar, M. Breeman, A. V. Mijiritskii, D. O. Boerma, *Nucl. Instrum. Methods B* **132**, 578 (1997), and references therein.
35. M. Copel, T. Gustafsson, W. R. Graham and S. M. Yalisove, *Phys. Rev. B* **33**, 8110 (1986).
36. J. Stensgaard, R. Feidenhans'l and J. E. Sørensen, *Surf. Sci.* **128**, 281 (1983).
37. F. Jona, P. Jiang and P. M. Marcus, *Surf. Sci.* **192**, 414 (1987).
38. D. L. Adams, H. B. Nielsen and J. N. Andersen, *Surf. Sci.* **128**, 294 (1983).
39. Th. Fauster, D. Hartwig and H. Dürr, *Appl. Phys. A* **45**, 63 (1988).
40. K. Broomfield, R. A. Stansfield and D. C. Clary, *Surf. Sci.* **202**, 320 (1988).
41. H. S. Tan and M. A. Karolewski, *Nucl. Instrum. Methods B* **73**, 163 (1993).
42. K. Nordlund, N. Runeberg and D. Sundholm, *Nucl. Instrum. Methods B* **132**, 45 (1997).



43. R. S. Daley, J. H. Huang and R. S. Williams, *Surf. Sci.* **215**, 281 (1989).
44. W. D. Roos, J. du Plessi, G. N. van Wyk, E. Taglauer and S. Wolf, *J. Vac. Sci. Technol. A* **14**, 1648 (1996).
45. C. C. Chang, *Surf. Interface Anal.* **15**, 79 (1990).
46. W. K. Way, A. C. Pike, S. W. Rosencrance, P. M. Braun and N. Winograd, *Surf. Interface Anal.* **24**, 137 (1996).
47. D. Onderlinden, *Can. J. Phys.* **46**, 739 (1968).
48. M. Hou and W. Eckstein, *Nucl. Instrum. Methods B* **13**, 393 (1986).
49. F. Karetta and H. M. Urbassek, *Appl. Phys. A* **55**, 364 (1992).
50. G. Betz and W. Husinsky, *Nucl. Instrum. Methods B* **102**, 281 (1995).
51. D. P. Jackson, *Surf. Sci.* **43**, 431 (1974).
52. M. Aono, Y. Hou, C. Oshima and Y. Ishizawa, *Phys. Rev. Lett.* **49**, 567 (1982).